INTERNATIONAL JOURNAL FOR NUMERICAL METHODS IN ENGINEERING, VOL. 23, 253–274 (1986)

A TOTAL LAGRANGIAN FORMULATION FOR THE GEOMETRICALLY NONLINEAR ANALYSIS OF STRUCTURES USING FINITE ELEMENTS. PART II: ARCHES, FRAMES AND AXISYMMETRIC SHELLS

J. OLIVER AND E. OÑATE

E. T. S. Ingenieros de Caminos, Jordi Girona Salgado, 31, 08034 Barcelona, Spain

INTRODUCTION

The analysis of shells, arches or frames experiencing large displacements and rotations is of considerable interest in many fields of civil, mechanical and aeronautical engineering. Several researchers have put much effort in the last few years to develop efficient finite element formulations which give accurate numerical solutions at a reasonable computer cost.[1–15] One of the first general formulations to treat axisymmetric shell and one-dimensional (1D) structural problems was proposed by Wood and Zienkiewicz.[4] They used a total Lagrangian approach with ϕ-linear 2D solid elements. However, such elements present ill-conditioning problems when used in the context of very thin structural applications. These problems have today been overcome by the development of new families of degenerated 1D axisymmetric and arch elements, which in most cases allow for shear deformation effects.[8,11,13,14] Recent contributions on the subject using an updated Lagrangian approach have been presented by Hughes[8,9] for 3D and 2D shell problems, and Cook[10] for the case of axisymmetric shells only. On the other hand, total Lagrangian formulations have also been recently suggested by Batoz and Jameaux[13] for beams and arches, and Surana[11,12] for general and axisymmetric shell cases.

In a previous paper,[15] the authors have presented an alternative total Lagrangian finite element formulation for the large displacement/large rotation analysis of 3D shell problems whose main features are: (a) degenerated 3D shell elements are used, (b) shear deformation effects are taken into account, (c) a local set of axes, based on the principal curvature directions, is used for the definition of strains and stresses, (d) zero elongation of the normal vector is implicity assured and (e) no restriction on the magnitude of the shell curvature is made. Accuracy of the formulation was checked on a wide range of examples.

The formulation presented in this paper can be considered as a special case of the more general one presented in Reference 15 for axisymmetric shell, arch and frame structures. The paper shows how the formulation can treat the three types of structures mentioned in a simple unified manner. Different alternatives for choosing the finite element interpolation to be used are presented and explicit forms of the most relevant finite element matrices are given. The accuracy of the formulation is checked in a series of examples where comparisons with results obtained with alternative formulations are shown. Finally, the formulation is used to analyse a problem of the laying of a waste-water marine pipeline, which shows the ability of the formulation to deal with this kind of practical problem.

0029–5981/86/030253–22$02.20

Received 25 May 1984
Revised 30 April 1985

GEOMETRIC DESCRIPTION

From now onwards, all details of the mathematical formulation will be presented in a unified manner for axisymmetric shells, arches and frames. We have to note that, throughout the analysis, the middle line of the structure will be assumed to be curved. However, the detailed form of the expressions for frames can be derived directly from those corresponding to arches, making in all terms the radius of curvature, R, equal to infinity.

A global co-ordinate system is chosen such that the plane which contains the middle line of the arch (or frame) coincides with the global plane xz. For axisymmetric shells the middle line of a generic meridional section is considered (see Figure 1).

Let $\mathbf{a}$ and $\mathbf{n}$ be unit vectors tangent and normal to the middle line at a generic point O, respectively. Parameters r and ϕ are defined as the arc length measured along the middle line and the angle between vector $\mathbf{a}$ and the global x axis, respectively (see Figure 2).

The components of vectors $\mathbf{a}$ and $\mathbf{n}$ can be written in matrix form as

$$\mathbf{a} = \begin{bmatrix} a_x \\ a_z \end{bmatrix} = \begin{bmatrix} \cos\phi \\ \sin\phi \end{bmatrix}; \quad \mathbf{n} = \begin{bmatrix} n_x \\ n_z \end{bmatrix} = \begin{bmatrix} -\sin\phi \\ \cos\phi \end{bmatrix} \tag{1}$$

Vectors $\mathbf{a}$ and $\mathbf{n}$ define at each point of the middle line a local co-ordinate system $x'z'$ (see Figure 2).

The position of a point P of the structure can be defined by a vector $\mathbf{r}$ such that, in matrix form,

$$\mathbf{r} = \begin{bmatrix} x \\ z \end{bmatrix} = \mathbf{r}_0 + t\mathbf{n} \tag{2}$$

where $\mathbf{r}_0$ is the position vector of the corresponding point O over the middle line and t is the distance between points O and P (see Figure 2).

From equations (1) and (2) can be found, using the relationships shown in Figure 2,

$$\begin{bmatrix} \dfrac{\partial(x,z)}{\partial(r,t)} \end{bmatrix} = \begin{bmatrix} \dfrac{\partial\mathbf{r}}{\partial r}, \dfrac{\partial\mathbf{r}}{\partial t} \end{bmatrix} = \mathbf{T}^{\mathrm{T}}\mathbf{R} \tag{3}$$

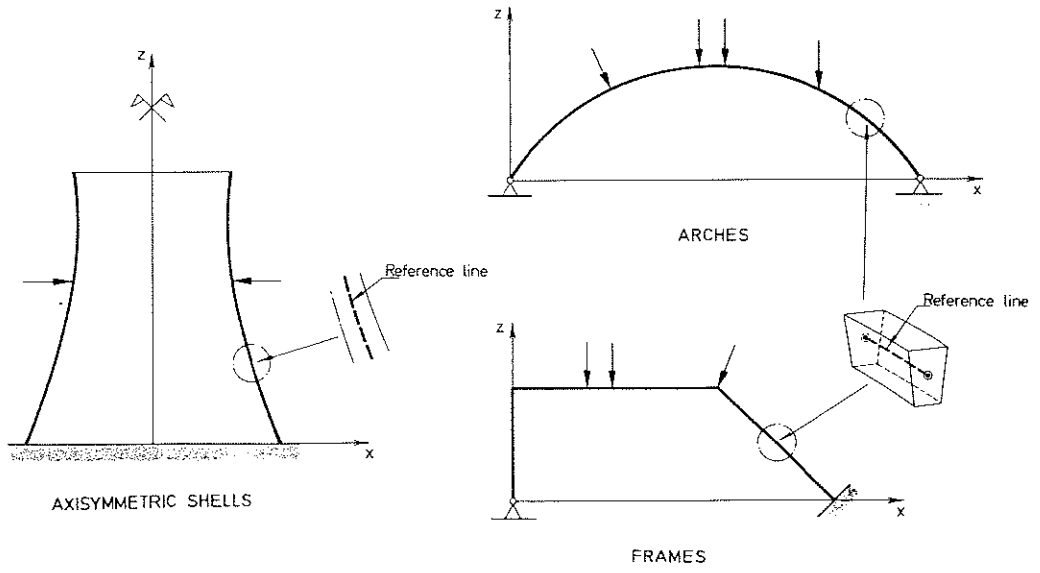

Figure 1. Different kinds of one-dimensional structures

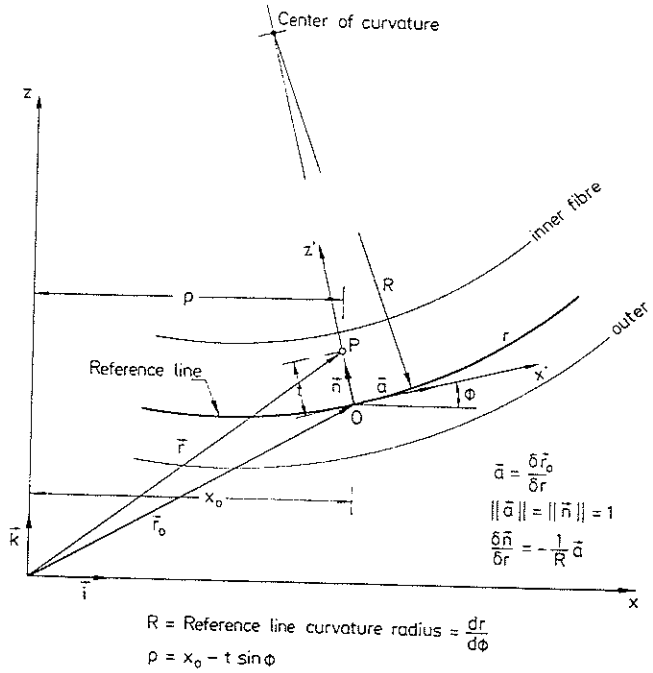

Figure 2. Geometric description

where $\mathbf{T}$ and $\mathbf{R}$ are defined by

$$\mathbf{T}=\left[\frac{\partial(x',z')}{\partial(x,z)}\right]=\begin{bmatrix}\cos\phi & \sin\phi\\ -\sin\phi & \cos\phi\end{bmatrix},\quad \mathbf{R}=\begin{bmatrix}1-(t/R) & 0\\ 0 & 1\end{bmatrix} \tag{4}$$

The middle line can be now approximated in an isoparametric form as

$$\mathbf{r}_0=\sum_1^{n_e} N_i(\xi)\mathbf{r}_{0_i} \tag{5}$$

where $\mathbf{r}_{0_i}$ is the position vector of node i of a mesh of one-dimensional finite elements discretizing the middle line of the structure (Figure 3a), $N_i(\xi)$ is the standard shape function of node i (Reference 16), ξ the normalized isoparametric co-ordinate and n_e the number of nodes of the element.

The second normalized co-ordinate τ is defined as

Arches/Frames

$$\tau=\frac{h_1-h_0+2t}{h}$$

Axisymmetric shells

$$\tau=\frac{2t}{h} \tag{6}$$

where h is the thickness of the structure, and distances h_0 and h_1 can be seen in Figure 3(a). From equation (2), (5) and (6) can be finally obtained

$$\mathbf{r}=\sum_1^{n_e} N_i(\xi)\mathbf{r}_{0_i}+\left(\tau\frac{h}{2}+\bar{h}\right)\mathbf{n} \tag{7}$$

where $\bar{h}=0$ or $\bar{h}=(h_0-h_1)/2$ for axisymmetric shells and arches, respectively.

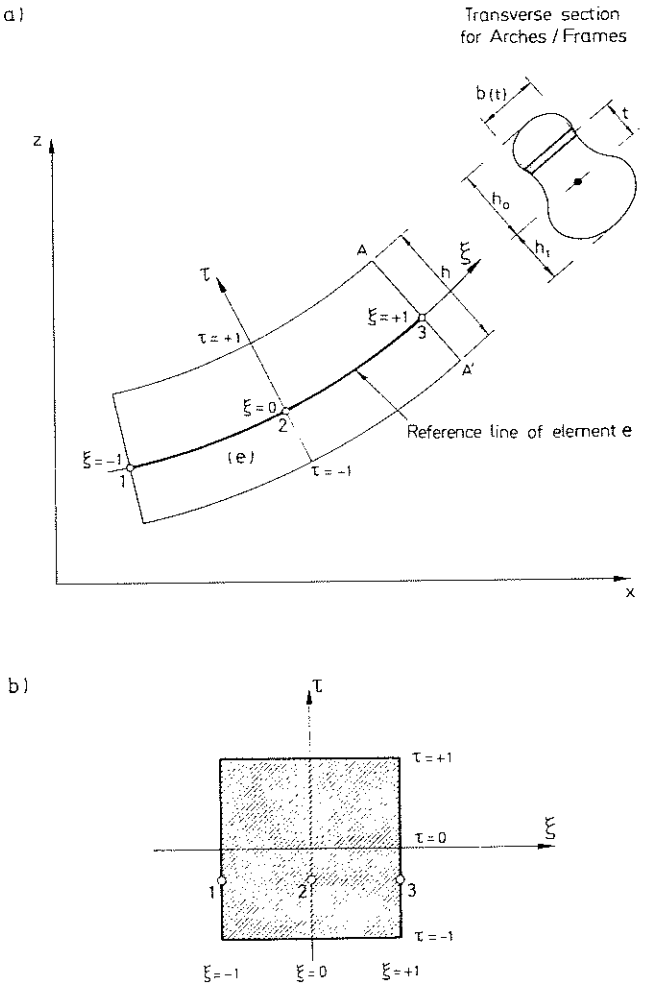

Figure 3. Discretization of the middle line into finite elements: (a) isoparametric 1D three-noded element; (b) normalized integration domain

Equation (7) transforms the area corresponding to an element into a square in the system ξ, τ (see Figure 3b).

KINEMATIC DESCRIPTION

The deformation of the structure is based on the following two main assumptions: (a) normals to the middle line before deformation remain straight but not necessarily normal to the middle line after deformation; (b) the length of the normal vector does not change during deformation.

Assumption (a) allows to express the displacement vector $\mathbf{u}$ of a generic point P, at a distance t from the corresponding point O over the middle line, as

$$\mathbf{u} = \mathbf{u}_0 + t\mathbf{u}_1 \tag{8}$$

where $\mathbf{u}_0$ is the displacement of point O and $\mathbf{u}_1$ is the displacement vector of the end of the normal

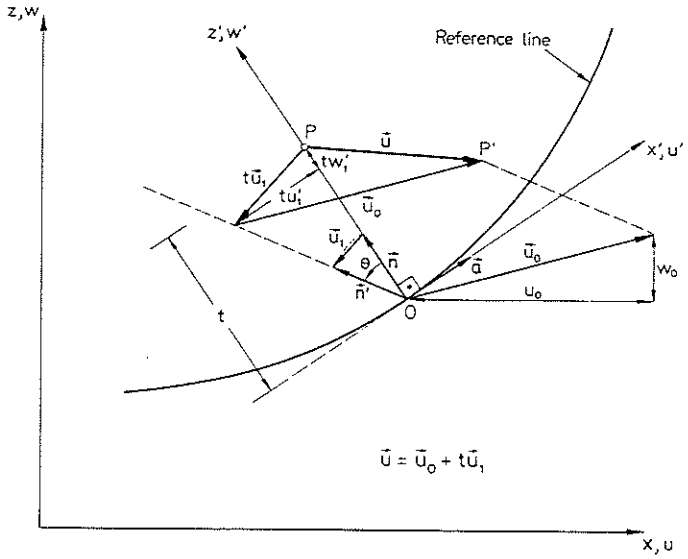

Figure 4. Kinematic description

vector in O (see Figure 4). The vector of *fundamental displacements* is defined now as

$$\mathbf{p} = [u_0, w_0, u'_1, w'_1]^T \tag{9}$$

where u_0 and w_0 are the components of $\mathbf{u}_0$ in the global system xz and u'_1, w'_1 are the components of $\mathbf{u}_1$ *in the local system* $x'z'$.

On the other hand, assumption (b) allows to express the displacements u'_1 and w'_1 as

$$\mathbf{u}'_1 = \begin{bmatrix} u'_1 \\ w'_1 \end{bmatrix} = \begin{bmatrix} -\sin\theta \\ \cos\theta - 1 \end{bmatrix} \tag{10}$$

where θ is the angle rotated by the normal vector during deformation. Equation (10) is the basis for obtaining alternative approximate (i.e. linearized) expressions for the rotation components of the displacement vector of equation (9). In this work the full form of equation (10) has been taken.

Finite element interpolation

There are several options for defining the finite element interpolation to be used. Among these we can note the following three options.

Option 1. The four components of vector $\mathbf{p}$ of equation (9) are interpolated, i.e.

$$\mathbf{p} = \sum_{i=1}^{n_e} \mathbf{N}_i \mathbf{p}_i \quad \text{with} \quad \mathbf{N}_i = N_i \mathbf{I}_4 \tag{11}$$

where $\mathbf{p}_i$ are the nodal values of p and $\mathbf{I}_4$ is the 4×4 unit matrix.

Option 2. The 'fundamental displacement' vector is redefined as

$$\hat{\mathbf{p}} = [u_0, w_0, u_1, w_1]^T \tag{12}$$

where u_1 and w_1 are the components of vector $\mathbf{u}_1$ in the *global system xz* given by

$$\begin{aligned} u_1 &= -\sin\theta\cos\phi - (\cos\theta - 1)\sin\phi \\ w_1 &= -\sin\theta\sin\phi + (\cos\theta - 1)\cos\phi \end{aligned} \tag{13}$$

Vector $\hat{\mathbf{p}}$ can now be interpolated as

$$\hat{\mathbf{p}} = \sum_{i=1}^{n_e} \mathbf{N}_i \hat{\mathbf{p}}_i \tag{14}$$

This option has been used by Surana in the context of axisymmetric shells.[11]

Option 3. The *vector of displacements* is defined as

$$\mathbf{a} = [u_0, w_0, \theta]^{\mathrm{T}} \tag{15}$$

Vector $\mathbf{a}$ can be interpolated as

$$\mathbf{a} = \sum_{i=1}^{n_e} \bar{\mathbf{N}}_i \mathbf{a}_i \quad \text{with} \quad \bar{\mathbf{N}}_i = N_i \mathbf{I}_3 \tag{16}$$

Use of one or other option leads to different finite element forms. It can be easily checked that option 1, defined by equation (11), leads to simpler mathematical expressions for the finite element matrices, and that option has been chosen in this paper.

STRAIN FIELD

Let $\mathbf{u}' = \{u', w'\}^{\mathrm{T}}$ be the vector containing the components of the displacement vector of a point P in the local system $x'z'$, defined in the corresponding point O over the middle line (see Figure 4), i.e.

$$\mathbf{u} = u'\mathbf{a} + w'\mathbf{n} \tag{17}$$

The vector of displacement gradients in P is defined by $\mathbf{g}$ with

Arches/Frames *Axisymmetric shells*

$$\mathbf{g}^A = \begin{bmatrix} \mathbf{g}_1 \\ \mathbf{g}_2 \end{bmatrix} \qquad \mathbf{g}^{AS} = \begin{bmatrix} \mathbf{g}^A \\ g_5 \end{bmatrix} \tag{18}$$

From now onwards superscripts A and AS will be used to specify the value of vectors and matrices for arches/frames and axisymmetric shells, respectively. In equation (18)

$$\mathbf{g}_1 = \begin{bmatrix} g_1 \\ g_2 \end{bmatrix} = \begin{bmatrix} \dfrac{\partial u'}{\partial x'} \\ \dfrac{\partial w'}{\partial x'} \end{bmatrix}; \quad \mathbf{g}_2 = \begin{bmatrix} g_3 \\ g_4 \end{bmatrix} = \begin{bmatrix} \dfrac{\partial u'}{\partial z'} \\ \dfrac{\partial w'}{\partial z'} \end{bmatrix} \tag{19}$$

and

$$g_5 = \frac{u}{\rho} \quad \rho = x_0 - t\sin\phi \quad \text{(see Figure 2)} \tag{20}$$

The Green strain vector $\boldsymbol{\varepsilon}$ (associated to the local directions $x'z'$) at P is defined by

Arches/Frames *Axisymmetric shells*

$$\boldsymbol{\varepsilon}^A = \begin{bmatrix} \varepsilon_{x'} \\ \gamma_{x'z'} \end{bmatrix} = \begin{bmatrix} g_1 + \frac{1}{2}(g_1^2 + g_2^2) \\ g_2 + g_3 + g_1 g_3 + g_2 g_4 \end{bmatrix} \qquad \boldsymbol{\varepsilon}^{AS} = \begin{bmatrix} \boldsymbol{\varepsilon}^A \\ \varepsilon_{y'} \end{bmatrix} = \begin{bmatrix} \varepsilon^A \\ g_5 + \frac{1}{2}g_5^2 \end{bmatrix} \tag{21}$$

It is shown in Appendix I that

$$\mathbf{g} = \mathbf{L}\mathbf{p} \tag{22}$$

where $\mathbf{p}$ is the fundamental displacement vector defined above and the strain operator $\mathbf{L}$ is given by

Arches/Frames *Axisymmetric shells*

$$\mathbf{L}^A = \begin{bmatrix} C_r \mathbf{T} \dfrac{\mathrm{d}}{\mathrm{d}r} & tC_r \left[\boldsymbol{\Delta} + \mathbf{I}_2 \dfrac{\mathrm{d}}{\mathrm{d}r} \right] \\ \mathbf{0} & \mathbf{I}_2 \end{bmatrix} \qquad \mathbf{L}^{AS} = \begin{bmatrix} \mathbf{L}^A \\ \dfrac{1}{\rho}, 0, \dfrac{t}{\rho}\cos\phi, -\dfrac{t}{\rho}\sin\phi \end{bmatrix} \tag{23}$$

with

$$\boldsymbol{\Delta} = \frac{1}{R}\begin{bmatrix} 0 & -1 \\ 1 & 0 \end{bmatrix} \qquad C_r = \frac{1}{1 - \dfrac{t}{R}} \tag{24}$$

(for frames $\boldsymbol{\Delta} = \mathbf{0}$ and $C_r = 1$)

At this point a decision about the finite element interpolation to be used should be taken. As previously mentioned, option 1 has been chosen for deriving the expressions shown next.

Substitution of equation (11) in equations (22) yields

$$\mathbf{g} = \mathbf{L} \sum_{i=1}^{n_e} \mathbf{N}_i \mathbf{p}_i = \sum_{i=1}^{n_e} \mathbf{M}_i \mathbf{p}_i \tag{25}$$

where $\mathbf{M}_i = \mathbf{L}^A \mathbf{N}_i$ or $\mathbf{L}^{AS}\mathbf{N}_i$ for arches and axisymmetric shells, respectively.

The full (nonlinearized) incremental form of equation (25) can be easily derived as

$$\delta \mathbf{g} = \sum_{i=1}^{n_e} \mathbf{M}_i \delta \mathbf{p}_i \tag{26}$$

On the other hand, from the definition of $\mathbf{p}$ (see equations (9) and (10)) it can be found:

$$\delta \mathbf{p}_i = \begin{bmatrix} 1 & 0 & 0 \\ 0 & 1 & 0 \\ 0 & 0 & -\cos\theta_i \\ 0 & 0 & -\sin\theta_i \end{bmatrix} \begin{bmatrix} \delta u_{0_i} \\ \delta w_{0_i} \\ \delta\theta_i \end{bmatrix} = \mathbf{C}_i \delta \mathbf{a}_i \tag{27}$$

Substitution of equation (27) in (26) yields

$$\delta \mathbf{g} = \sum_{i=1}^{n_e} \mathbf{M}_i \mathbf{C}_i \delta \mathbf{a}_i = \sum_{i=1}^{n_e} \mathbf{G}_i \delta \mathbf{a}_i \tag{28}$$

where matrix $\mathbf{G}_i$ can be explicitly obtained as

Arches/Frames

$$\underset{4\times 3}{\mathbf{G}_i^A} = \left[\begin{array}{c|c} C_r \dfrac{\mathrm{d}N_i}{\mathrm{d}r} \underset{2\times 2}{\mathbf{T}} & \begin{matrix} -tC_r \left[\dfrac{\mathrm{d}N_i}{\mathrm{d}r}\cos\theta_i - \dfrac{N_i}{R}\sin\theta_i \right] \\ -tC_r \left[\dfrac{\mathrm{d}N_i}{\mathrm{d}r}\sin\theta_i + \dfrac{N_i}{R}\cos\theta_i \right] \end{matrix} \\ \hline \underset{2\times 2}{\mathbf{0}} & \begin{matrix} -N_i\cos\theta_i \\ -N_i\sin\theta_i \end{matrix} \end{array}\right] \tag{29}$$

Axisymmetric shells

$$\underset{5\times 3}{\mathbf{G}_i^{AS}} = \begin{bmatrix} & \mathbf{G}_i^{A} & \\ \dfrac{N_i}{\rho}, & 0, & -\dfrac{tN_i}{\rho} \quad [\cos\phi\cos\theta_i - \sin\phi\sin\theta_i] \end{bmatrix} \tag{30}$$

From equations (21) it can be easily found

$$\delta\boldsymbol{\varepsilon} = \mathbf{A}\delta\mathbf{g} \tag{31}$$

where matrix $\mathbf{A}$ is given by

Arches/Frames

$$\mathbf{A}^{A} = \begin{bmatrix} (1+g_1) & g_2 & 0 & 0 \\ g_3 & (1+g_4) & (1+g_1) & g_2 \end{bmatrix}$$

Axisymmetric shells

$$\mathbf{A}^{AS} = \begin{bmatrix} \mathbf{A}^{A} & \mathbf{0} \\ \mathbf{0} & 1+g_5 \end{bmatrix} \tag{32}$$

Finally, substituting equation (28) in (31) it can be obtained

$$\delta\boldsymbol{\varepsilon} = \mathbf{A}\sum_{i=1}^{n_e}\mathbf{G}_i\delta\mathbf{a}_i = \sum_{i=1}^{n_e}\mathbf{B}_i\delta\mathbf{a}_i \tag{33}$$

An explicit form of matrix $\mathbf{B}_i$ for arches and axisymmetric shells is given in Table I.

Table I. Matrix $\mathbf{B}_i$ for arches/frames and axisymmetric shells (option 1)

Arches/Frames

$$\mathbf{B}_i^{A} = \left[\begin{array}{c|c|c} C_r\dfrac{dN_i}{dr}[(1+g_1)\cos\phi - g_2\sin\phi] & C_r\dfrac{dN_i}{dr}[(1+g_1)\sin\phi + g_2\cos\phi] & -C_r t[(1+g_1)A_i + g_2 B_i] \\ \hline C_r\dfrac{dN_i}{dr}[g_3\cos\phi - (1+g_4)\sin\phi] & C_r\dfrac{dN_i}{dr}[(g_3\sin\phi + (1+g_4)\cos\phi] & \begin{array}{l} -tC_r[g_3 A_i + (1+g_4)] - \\ -N_i[(1+g_1)\cos\theta_i \\ \quad + g_2\sin\theta_i] \end{array} \end{array}\right]$$

Axisymmetric shells

$$B_i^{AS} = \left[\begin{array}{c|c|c} & \mathbf{B}_i^{A} & \\ \hline \dfrac{N_i}{\rho}(1+g_5) & 0 & -\dfrac{tN_i}{\rho}(1+g_5)(\cos\phi\cos\theta_i - \sin\phi\sin\theta_i) \end{array}\right]$$

$$A_i = \frac{dN_i}{dr}\cos\theta_i - \frac{N_i}{R}\sin\theta_i \qquad C_r = \frac{1}{1-\dfrac{t}{R}}$$

$$B_i = \frac{dN_i}{dr}\sin\theta_i + \frac{N_i}{R}\cos\theta_i \qquad \rho = x - t\sin\phi$$

(For frames $1/R = 0$ in the above relations)

CONSTITUTIVE EQUATIONS

We will not go into details of the different constitutive equations which could be used for nonlinear analysis of the structures studied in this paper. It will simply be assumed that an increment relationship between the second Piola–Kirchhoff stress vector, $\boldsymbol{\sigma}$, and the Green strain vector of equation (21) can be found in the form

$$\delta\boldsymbol{\sigma} = \mathbf{D}\delta\boldsymbol{\varepsilon} \tag{34}$$

where $\boldsymbol{\sigma}$ is given by (see Figure 5)

Arches/Frames $\qquad\qquad$ *Axisymmetric shells*

$$\boldsymbol{\sigma}^{A} = [\sigma_x, \tau_{x'z'}]^{\mathrm{T}} \qquad \boldsymbol{\sigma}^{AS} = [\sigma_{x'}, \tau_{x'z'}, \sigma_{y'}]^{\mathrm{T}} \tag{35}$$

For linear elastic materials, matrix $\mathbf{D}$ is given by

$$\mathbf{D}^{A} = E\begin{bmatrix} 1 & 0 \\ 1 & \dfrac{1}{2(1+\nu)} \end{bmatrix} \qquad \mathbf{D}^{AS} = \frac{E}{1-\nu^2}\begin{bmatrix} 1 & 0 & \nu \\ 0 & \dfrac{1-\nu}{2} & 0 \\ \nu & 0 & 1 \end{bmatrix} \tag{36}$$

Other different forms of matrix $\mathbf{D}$ for nonlinear material behaviour can be found in Reference 17.

DISCRETIZED EQUILIBRIUM EQUATIONS

The discretized finite element equations are obtained via the virtual work expression in its Lagrangian form.[16] A typical equations for the ith node is usually written as

$$\boldsymbol{\psi}_i(\mathbf{a}) = \int_V \mathbf{B}_i^{\mathrm{T}}\boldsymbol{\sigma}\mathrm{d}V - \bar{\mathbf{R}}_i(\mathbf{a}) = \mathbf{0} \tag{37}$$

where V is the volume of the structure, $\boldsymbol{\psi}_i(\mathbf{a})$ is the residual force vector and $\bar{\mathbf{R}}_i(\mathbf{a})$ is the equivalent nodal force vector due to exterior loads. For conservative loading $\bar{\mathbf{R}}_i(\mathbf{a}) = \mathbf{R}_i$. Typical examples of vector $\mathbf{R}_i$ are the following.

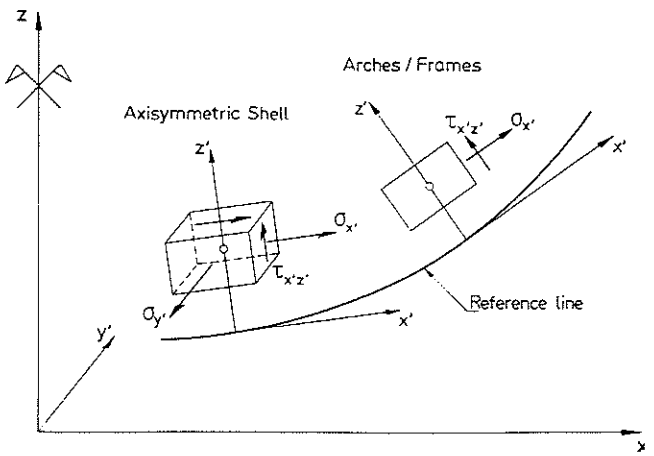

Figure 5. Definition of local second Piola–Kirchhoff stresses

Point loads

$$\mathbf{R}_i = \beta_i [f_{x_i}, f_{z_i}, M_i]^{\mathrm{T}} \tag{38}$$

where f_{x_i} and f_{z_i} are the point load components in the global directions x, z, respectively, acting at node i, M_i is the external bending moment applied at that node and $\beta_i = 1$ and $\beta_i = 2\pi x_i$ for arches and axisymmetric shells, respectively. Note that for axisymmetric shells the components of vector $\mathbf{R}_i$ refer to its circumferential values uniformly distributed along a circumference of radius x_i.

Distributed loads

$$\mathbf{R}_i = \int_{1^{(e)}} [N_i t_x, N_i t_z, 0]^{\mathrm{T}} \beta \mathrm{d}r \tag{39}$$

where t_x and t_z are the load intensities, acting per unit length of the middle line along directions x and z, respectively, and $\beta = 1$ and $2\pi x$ for arches and axisymmetric shells, respectively. Again, for axisymmetric shells the components of the load refer to circumferential values.

Self-weight

$$\mathbf{R}_i = -\int_V [0, N_i, 0]^{\mathrm{T}} \bar{\rho} g \mathrm{d}V \tag{40}$$

where $\bar{\rho}$ is the material density and g the value of gravity (assumed to act in opposite direction to the z axis).

Obtention of the tangent matrix

Equation (37) is a nonlinear system of equations which can be solved using any of the existing procedures developed for that purpose.[18] In this work a standard Newton–Raphson algorithm has been chosen. This gives for the nth displacement increment

$$\Delta \mathbf{a}^n = -\mathbf{K}_{\mathrm{T}}(\mathbf{a}^n) \boldsymbol{\psi}(\mathbf{a}^n) \tag{41}$$

from which the value of $\mathbf{a}^{n+1}$ can be found as $\mathbf{a}^{n+1} = \mathbf{a}^n + \Delta \mathbf{a}^n$.

A typical submatrix of the tangent matrix relating nodes i and j, is obtained by:[16]

$$\mathbf{K}_{T_{ij}}(\mathbf{a}) = \frac{\partial \boldsymbol{\psi}_i(\mathbf{a})}{\partial a_j} = \frac{\partial}{\partial a_j} \left\{ \int_V \mathbf{B}_i^{\mathrm{T}} \boldsymbol{\sigma} \mathrm{d}V \right\} - \frac{\partial}{\partial a_j} \bar{\mathbf{R}}_i(\mathbf{a}) \tag{42}$$

Equation (42) yields, for conservative loading,

$$\mathbf{K}_{T_{ij}}(\mathbf{a}) = \frac{\partial}{\partial a_j} \left\{ \int_V \mathbf{B}_i^{\mathrm{T}} \boldsymbol{\sigma} \mathrm{d}V \right\} = \mathbf{K}_{ij}^{\mathrm{L}} + \mathbf{K}_{ij}^{\sigma I} + \mathbf{K}_{ij}^{\sigma II} \tag{43}$$

where

$$\mathbf{K}_{ij}^{L} = \int_V \mathbf{B}_i^{\mathrm{T}} \mathbf{D} \mathbf{B}_j \mathrm{d}V \tag{44}$$

$$\mathbf{K}_{ij}^{\sigma I} = \int_V \mathbf{G}_i^{\mathrm{T}} \mathbf{S} \mathbf{G}_j \mathrm{d}V \tag{45}$$

and

$$\mathbf{K}_{ij}^{\sigma II} = \mathbf{0} \quad \text{for} \quad i \neq j \qquad \mathbf{K}_{ii}^{\sigma II} = \begin{bmatrix} 0 & 0 & 0 \\ 0 & 0 & 0 \\ 0 & 0 & H_i \end{bmatrix} \tag{46}$$

In equations (44), (45) and (46) all matrices and constants have been defined before except matrix S and H_i which are given by

Arches/Frames *Axisymmetric shells*

$$\underset{4\times4}{\mathbf{S}^{A}} = \begin{bmatrix} \sigma_{x'}\mathbf{I}_2 & \tau_{x'z'}\mathbf{I}_2 \\ \tau_{x'z'}\mathbf{I}_2 & \mathbf{0} \end{bmatrix} \qquad \underset{5\times5}{\mathbf{S}^{AS}} = \begin{bmatrix} \mathbf{S}^{A} & \mathbf{0} \\ \mathbf{0} & \sigma_{y'} \end{bmatrix} \tag{47}$$

$$\begin{aligned} H_i^A = &-(1+g_1)(G_{23_i}\sigma_{x'} + G_{43_i}\tau_{x'z'}) \\ &+ g_2(G_{13_i}\sigma_{x'} + G_{33_i}\tau_{x'z'}) \\ &- g_3 G_{23_i}\tau_{x'z'} \\ &+ (1+g_4)G_{13_i}\tau_{x'z'} \end{aligned} \qquad H_i^{AS} = H_i^A + (1+g_5)\frac{\partial G_{53_i}}{\partial \theta_i}\sigma_{y'} \tag{48}$$

where $G_{13_i}, \ldots, G_{53_i}$ are the components of the last column of matrix $\mathbf{G}_i$ and

$$\frac{\partial G_{53_i}}{\partial \theta_i} = \frac{tN_i}{\rho}(\cos\phi\sin\theta_i + \sin\phi\cos\theta_i) \tag{49}$$

NUMERICAL INTEGRATION AND FINITE ELEMENT CHOSEN

All integrals have been evaluated using a Gauss–Legendre numerical integration rule. It is easy to shown that the differential of volume can be expressed in the normalized system ξ, τ by the following expression:

$$dV = b(t)\left(1 - \frac{t}{R}\right)\frac{h}{2}\left[\left(\frac{dx_0}{d\xi}\right)^2 + \left(\frac{dz_0}{d\xi}\right)^2\right]^{1/2} d\xi d\tau \tag{50}$$

where the index 0 denotes points of the middle line, t is the co-ordinate along the thickness direction, h the thickness of the element and

$b(t)$ = width of the transverse section at the fibre of co-ordinate t, for *arches and frames* (see Figure 3a);
$b(t) = 2\pi\rho$ for *axisymmetric shells.*

Equation (50) transforms the integration domain into the normalized square of Figure 3(b).

With regard to the type of element to be used, any of the one-dimensional elements recently developed to deal with 'thick' formulations for the type of structures presented in this paper could be adequate. For the examples presented in next section an isoparametric one-dimensional three-noded element (Figure 3a) has been chosen with the following reduced integration scheme: (a) reduced integration (2 Gauss–Legendre integration points for all terms of matrix $\mathbf{K}_T$) along the ξ direction over the middle line of the structure; (b) two-point rule for the integration along the thickness (τ) direction.

EXAMPLES

Example 1. Expansion bellow under end circular point load

The first example chosen to test the formulation is the analysis of a segment of an expansion bellow under circular point load acting at both ends. Figure 6 shows the cross-section of the

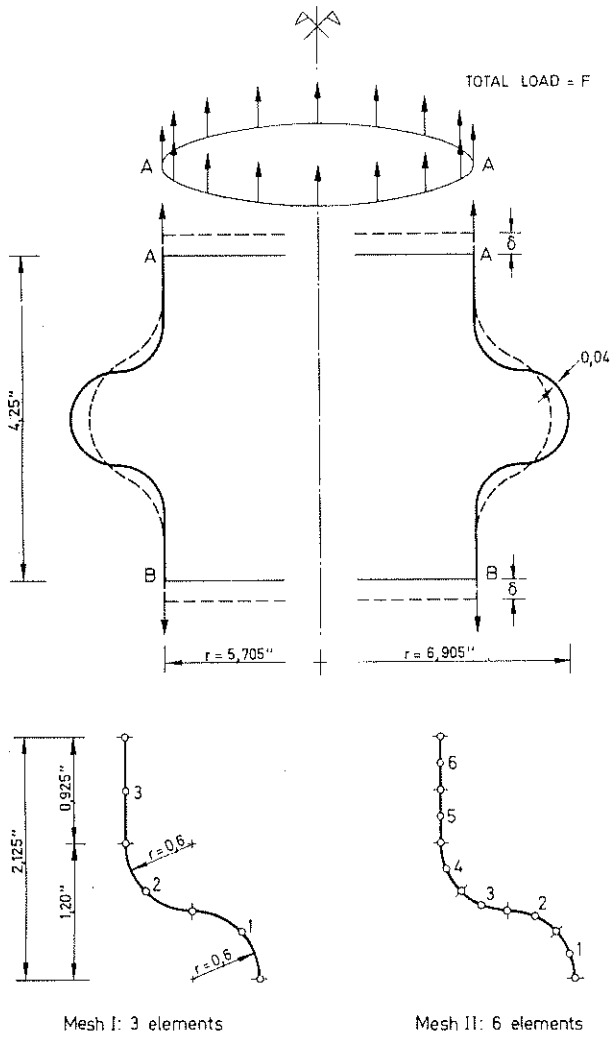

Figure 6. Expansion bellow under end circular point load: geometry, material properties and finite element meshes

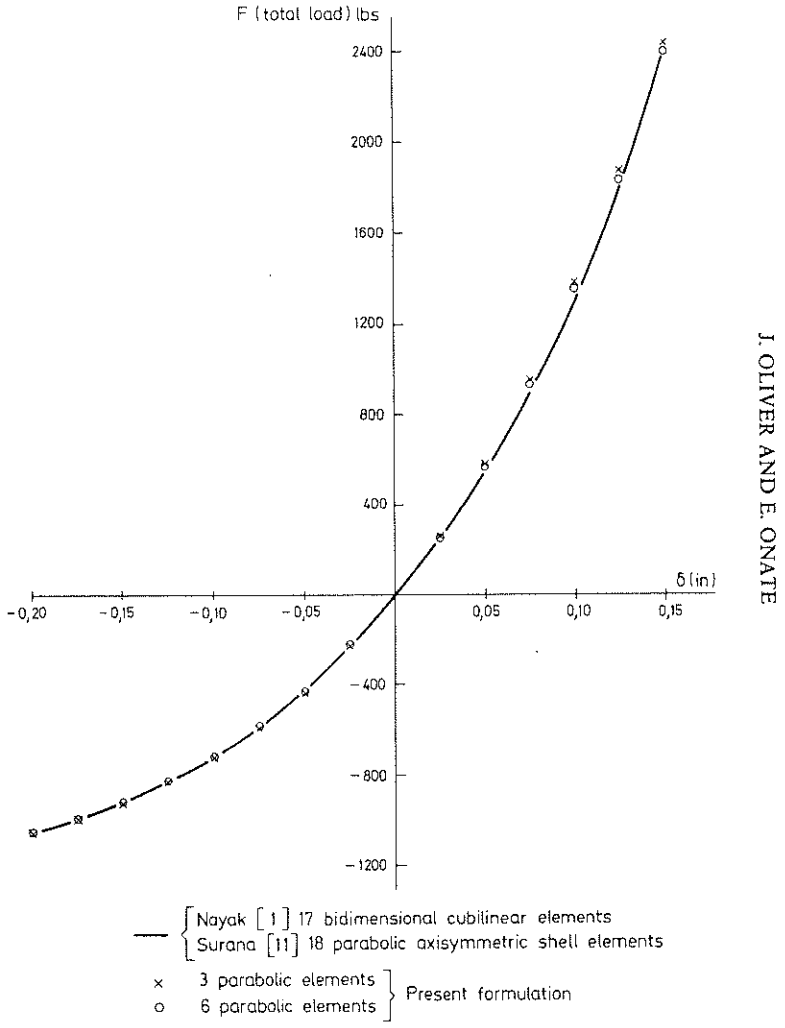

Figure 7. Expansion bellow under end circular point load: numerical results

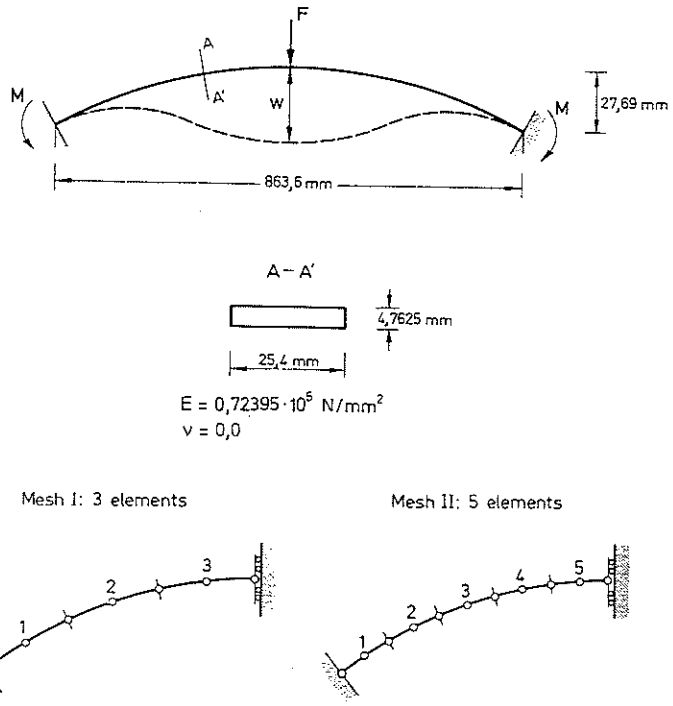

Figure 8. Clamped shallow circular arch. Geometry, material properties and finite element meshes

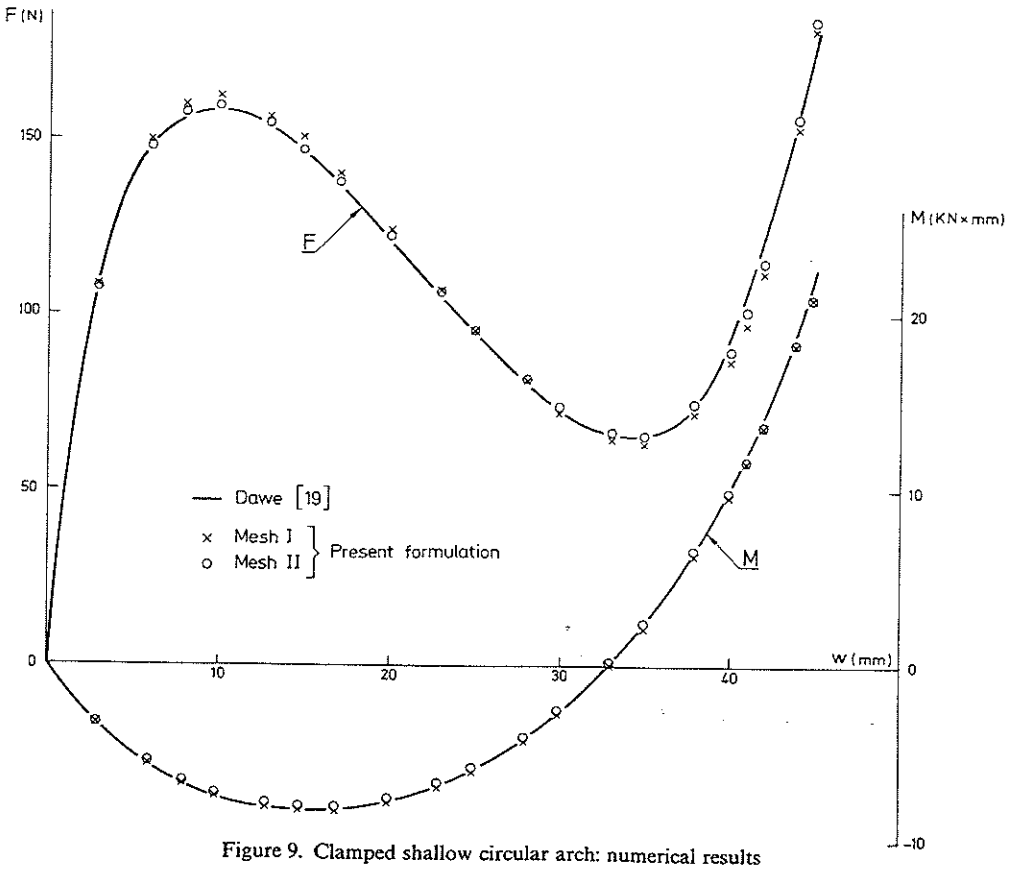

Figure 9. Clamped shallow circular arch: numerical results

segment analysed. The problem has been studied with two meshes of 3 and 6 parabolic axisymmetric shell elements also shown in Figure 6, together with the material properties used in the analysis. Results for the load–deflection curve have been obtained by applying equal increments of the vertical displacement, δ, at the end A. It can be seen in Figure 7 that numerical results obtained with the mesh of only 3 parabolic elements are very accurate in comparison with those obtained by Nayak[1] and Surana,[11] shown in the same figure, using a considerable higher number of elements.

Example 2. Clamped shallow circular arch under vertical point load

The geometry of the arch, material properties and two finite element meshes, of three and five isoparametric parabolic one-dimensional elements, respectively, used in the analysis are shown in

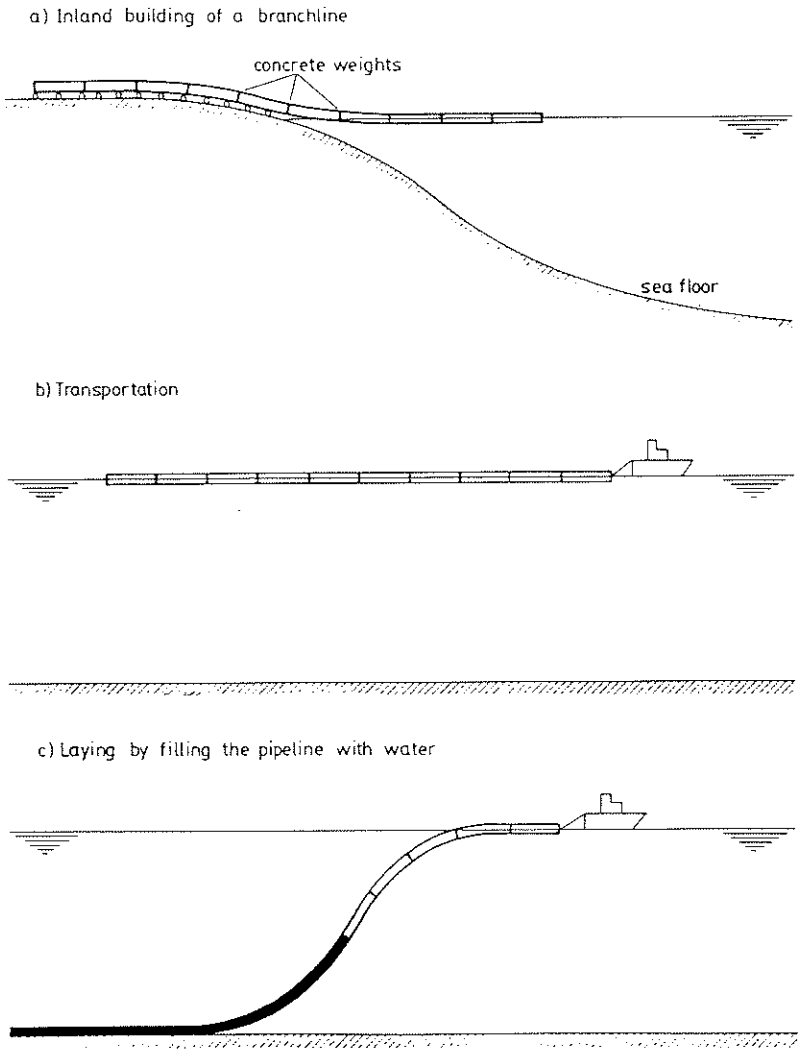

Figure 10. Different phases in the laying of marine pipelines from the sea surface by the method of continuous filling with water

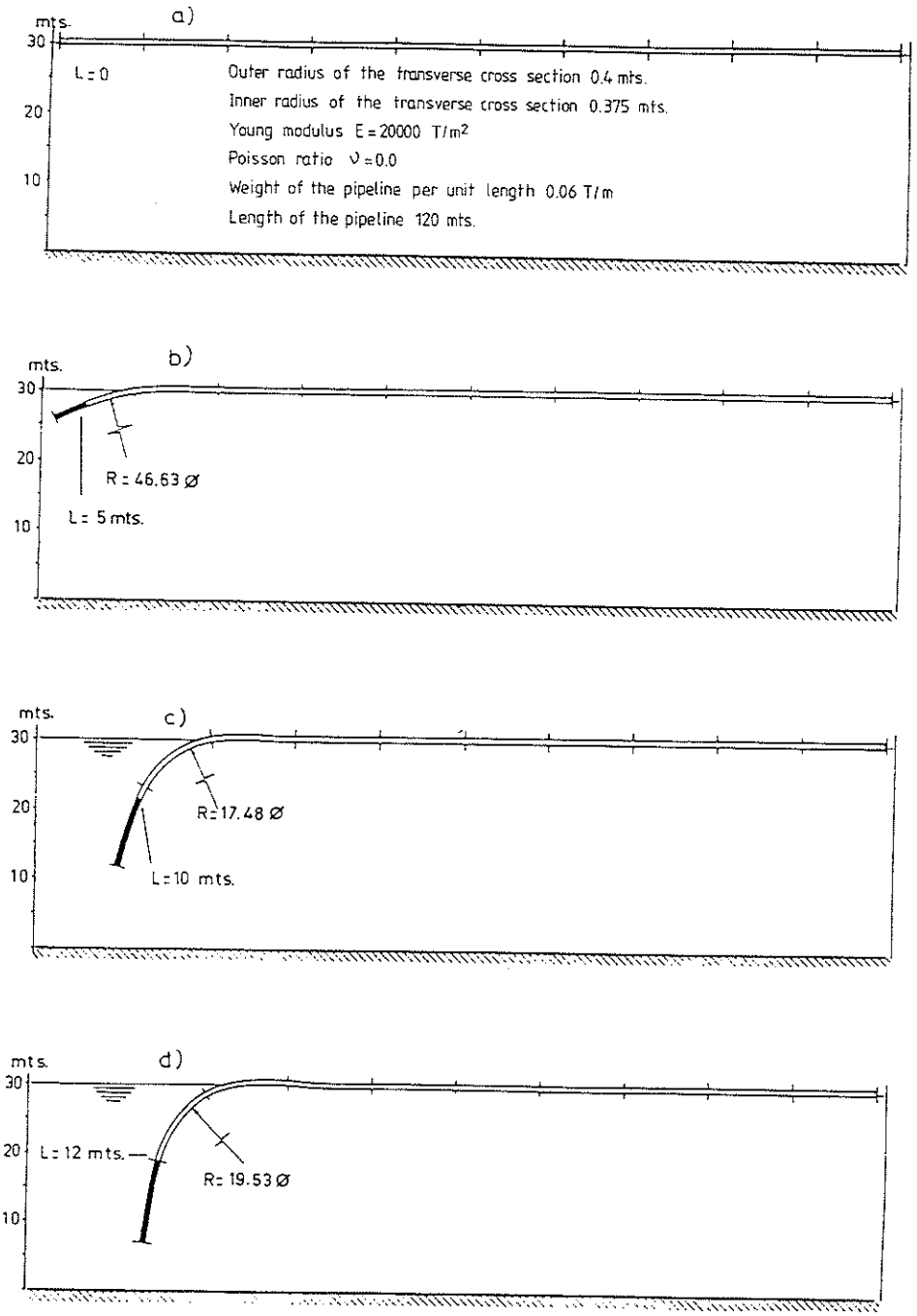

L = length of water inside the pipeline; ϕ = pipeline diameter
R = minimum radius of curvature

Figure 11. Deformed shape of the pipeline at various stages of the laying operation ($0 < L < 12$ m)

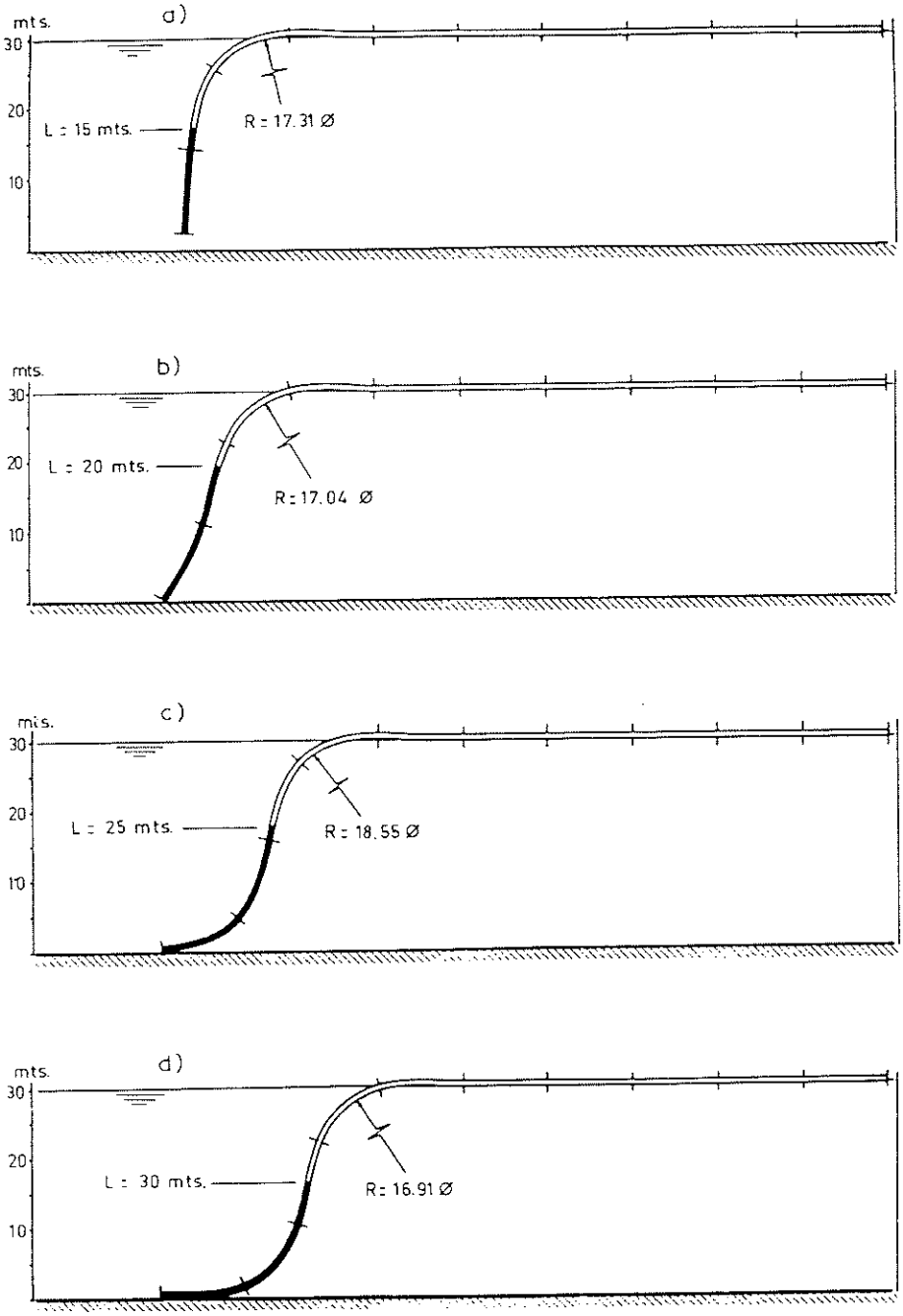

L = length of water inside the pipeline; ϕ = pipeline diameter
R = minimum radius of curvature

Figure 12. Deformed shape of the pipeline at various stages of the laying operation (15 m < L < 30 m)

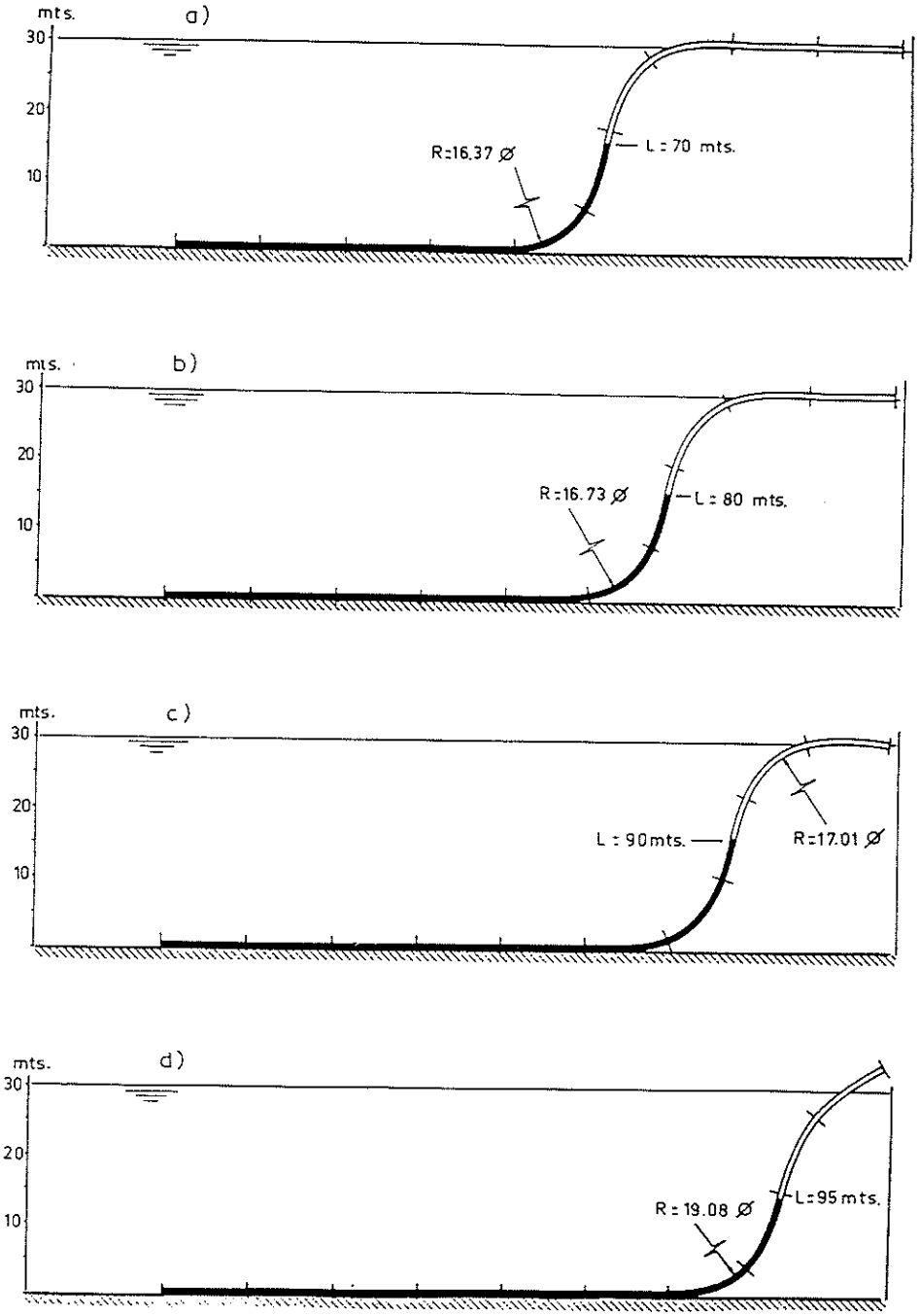

L = length of water inside the pipeline; ϕ = pipeline diameter
R = minimum radius of curvature

Figure 13. Deformed shape of the pipeline at various stages of the laying operation (70 m < L < 95 m)

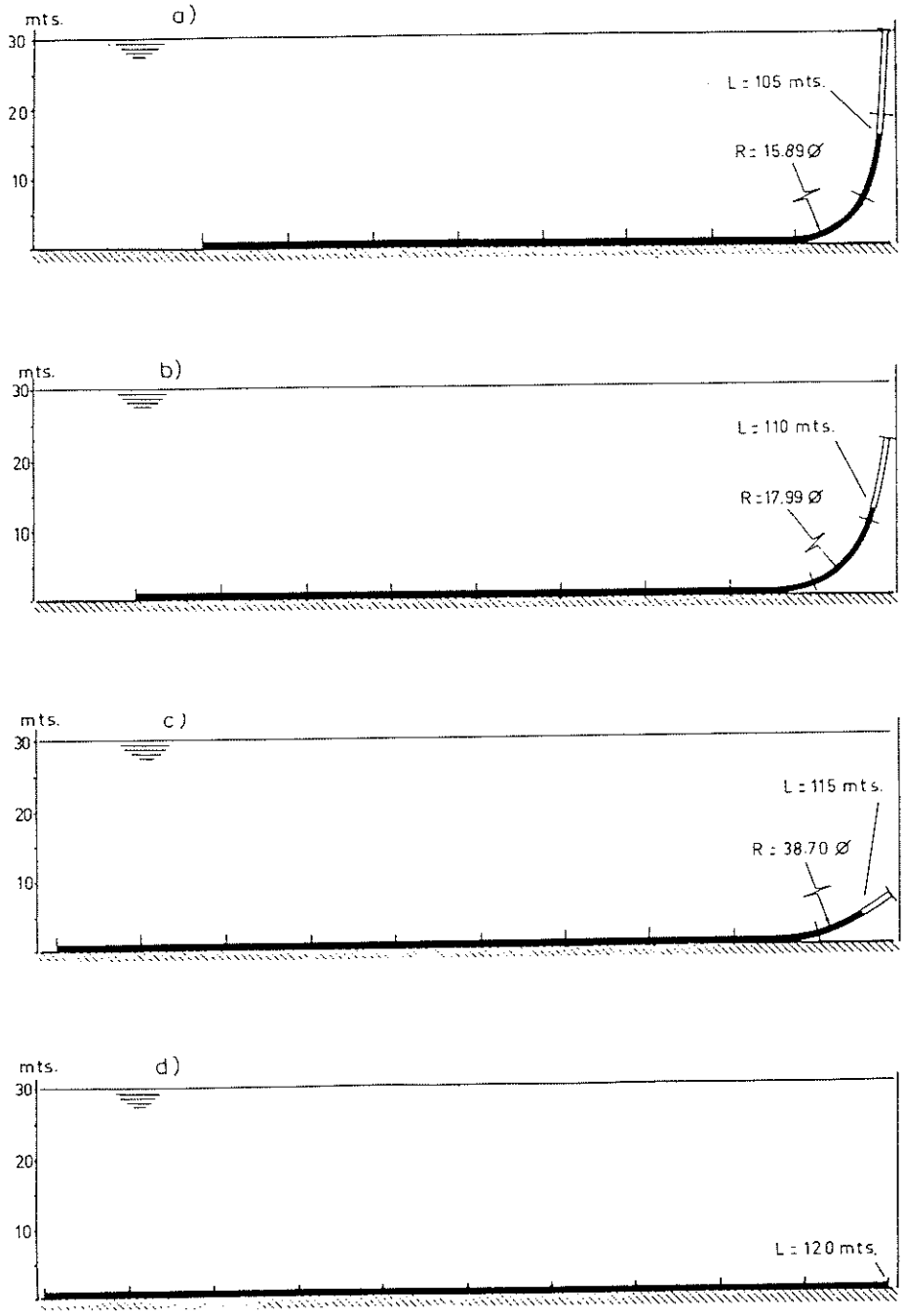

L = length of water inside the pipeline; ϕ = pipeline diameter
R = minimum radius of curvature

Figure 14. Deformed shape of the pipeline at various stages of the laying operation (105 m < L < 120 m)

Figure 8. Numerical results obtained for the applied load versus central deflection curve have been plotted in Figure 9. Results for the clamped end bending moment versus central deflection curve are shown in the same figure. Comparison of results with those obtained by Dawe,[19] also plotted in Figure 9, is good.

Example 3. Analysis of the deformation of a waste-water marine pipeline during laying operations

Marine pipeline laying operations are typical examples of large deflection problems, in which large rotations are involved, that can be easily treated with the arch formulation presented in this paper. The problem studied here is the analysis of the deformation of a polyethylene waste-water pipeline laid over the sea floor by a method consisting in progressively filling with water the interior of the pipe. The pipeline, which originally floats over the sea surface, has a number of concrete weights uniformly distributed along its length for stability reasons. A global description of the problem can be seen in Figure 10. More details can be found in Reference 20.

The geometrical and material properties of the problem are shown in Figure 11(a). The concrete weights have been simulated by an equivalent weight of 0·20833 T/m acting uniformly per unit length of pipeline. Ten isoparametric parabolic one-dimensional elements have been used in the analysis.

The problem has been solved by incrementing the amount of water filling the pipeline in a way such that the results obtained at the end of each water increment have been taken as the starting point for the new increment. It is worth noting that this method does not imply the change of the reference surface which is kept constant throughout the analysis and equal to the horizontal position of the pipeline at the onset of the first water increment. To solve the problem of contact between pipeline and sea floor, a trial solution iterative scheme has been used.[20,21] Numerical results for the deformation of the pipeline at different laying stages have been plotted in Figures 11–14. It has been checked that the numerical model simulates well many real phenomena, which occur in the practice of this type of problems, like the small lifting of the floating portion of the pipeline in the vicinity of the non-submerged region, the development and propagation of uniform wavy shape as the pipeline comes into contact with the floor, and the sudden lifting up and sinking when the whole pipeline is filled with water. Moreover, the model allows to predict accurately the zone of minimum curvature radius which is a parameter of paramount importance for the adequate design of the laying operation. Results obtained for similar problems, like that of the prediction of deflections and internal forces in steel pipelines during lay barge installation,[20,21] show that the formulation could be successfully used for obtaining accurate information to establish the optimal conditions for a wide range of marine pipeline laying problems.

CONCLUSIONS

A geometrically nonlinear finite element formulation based on a total Lagrangian approach for axisymmetric shells, arches and frames has been presented. The formulation allows for large displacement–large rotations of the structure. Shear deformation effects have also been taken into account. It has been shown how the formulation can be presented in a unified manner to treat simultaneously the three types of structures.

The discussion of the different alternatives for choosing the finite element interpolation parameters has shown that the interpolation based on the local components of the rotation of the normal vector yields simpler explicit forms for the finite element matrices. Accuracy and versatility of the formulation has been shown in a series of examples of application where numerical results

obtained compare very favourably with those obtained using other existing alternative formulations. Finally, the formulation presented seems very adequate to analyse the deformation of marine pipelines during laying operations.

APPENDIX I: COMPUTATION OF THE L OPERATOR

Let P be the point in which the $\mathbf{L}$ operator is to be calculated, and O the corresponding point over the middle line in which vectors $\mathbf{a}_0$ and $\mathbf{n}_0$ and the local system of co-ordinate $x'z'$ are defined (see Figure 15).

Let Q be another point laying over the normal $\mathbf{n}$ at a distance t^* from its corresponding point M over the middle line.

Finally let

$$\bar{\mathbf{u}}'_Q = \bar{\mathbf{u}}'_M + t^* \bar{\mathbf{u}}'_{1_M} \tag{51}$$

be the displacement vector of point Q *in the system* $x'z'$ *associated at point* O.

It is easy to show, using equations (3) and (4), that

$$[\mathbf{g}_1, \mathbf{g}_2]_P = \left[\frac{\partial(\bar{u}', \bar{w}')}{\partial(x', z')}\right]_P = \left[\frac{\partial(\bar{u}', \bar{w}')}{\partial(r, t)}\right]_P \mathbf{R}^{-1} \tag{52}$$

i.e.

$$\mathbf{g}_1 = C_r \left[\frac{\partial \bar{\mathbf{u}}'_Q}{\partial r}\right]_P \quad \text{and} \quad \mathbf{g}_2 = \left[\frac{\partial \bar{\mathbf{u}}'_Q}{\partial t}\right]_P \tag{53}$$

where subscript P denotes values at point P.

On the other hand, we can write

$$\begin{aligned} \mathbf{u}_M &= \bar{u}'_M \mathbf{a}_0 + \bar{w}'_M \mathbf{n}_0 \\ \mathbf{u}_{1_M} &= \bar{u}'_{1_M} \mathbf{a}_0 + \bar{w}'_{1_M} \mathbf{n}_0 = u'_{1_M} \mathbf{a} + w'_{1_M} \mathbf{n} \end{aligned} \tag{54}$$

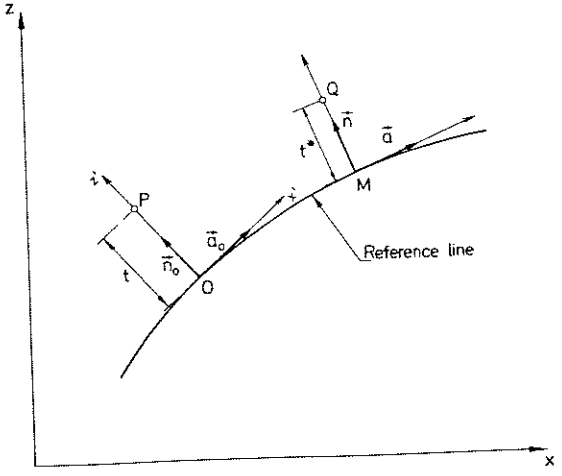

Figure 15

and consequently

$$\bar{\mathbf{u}}'_M = \begin{bmatrix} \mathbf{a}_0^T \\ \mathbf{n}_0^T \end{bmatrix} \cdot \mathbf{u}_M = \mathbf{T}_0 \mathbf{u}_M \tag{55}$$

$$\bar{\mathbf{u}}'_{1_M} = \begin{bmatrix} \mathbf{a}_0^T \\ \mathbf{n}_0^T \end{bmatrix} [\mathbf{a}, \mathbf{n}] \mathbf{u}'_{1_M} = \mathbf{T}_0 [\mathbf{a}, \mathbf{n}] \mathbf{u}'_{1_M} \tag{56}$$

where $\mathbf{u}_M$ denote components in the global system xz, $\mathbf{u}'_{1_M}$ denote components in the global system $\mathbf{a}, \mathbf{n}$ (associated at point M), and T_0 is the transformation matrix $\mathbf{T}$ defined in equation (4) particularized at point O.

Substituting in (51), (55) and (56) in (53) it can be obtained

$$\mathbf{g}_1 = C_r \mathbf{T}_0 \frac{d\mathbf{u}_0}{dr} + C_r t \left[\Delta \mathbf{u}'_1 + \mathbf{I}_2 \frac{d\mathbf{u}'_1}{dr} \right]$$

$$\mathbf{g}_2 = \mathbf{I}_2 \mathbf{u}'_1 \tag{57}$$

where $\mathbf{u}_0$ is the global (xz) displacement of point O, $\mathbf{u}'_1$ is the local $(x'z')$ displacement due to rotation of the normal in point O, and matrix Δ is shown in equation (24). From equations (57) the $\mathbf{L}^A$ operator for arches of equation (23) is automatically deduced.

For axisymmetric shells, we need to express g_5 of equation (19) in function of vector $\mathbf{p}$. From the expression

$$\mathbf{u}_1 = u'_1 \mathbf{a} + w'_1 \mathbf{n} \quad \text{or} \quad \mathbf{u}_1 = T^T \mathbf{u}'_1 \tag{58}$$

is possible to obtain, using explicit forms of matrix $\mathbf{T}$ in (4),

$$u_1 = \cos \phi u'_1 - \sin \phi w'_1 \tag{59}$$

and consequently

$$g_5 = \frac{u}{\rho} = \frac{u_0 + t u_1}{\rho} = \frac{u_0}{\rho} + \frac{t}{\rho} (\cos \phi u'_1 - \sin \phi w'_1) \tag{60}$$

From equations (60) the operator, $\mathbf{L}^{AS}$ of equation (23) can be automatically deduced.

REFERENCES

1. G. CH. Nayak, 'Plasticity and large deformation problems by the finite element method', *C/Ph/15/71*, Univ. of Wales, Swansea (1971).
2. O. C. Zienckiewicz and G. Ch. Nayak, 'A general approach to problems of large deformation and plasticity using isoparametric elements', *3rd. Conf. on Matrix Methods in Struct. Mech.*, A.F.I.T., Wright-Patterson Base, Ohio (October 1971).
3. R. D. Wood, 'The application of finite element methods to geometrically non-linear structural analysis', *C/Ph/20/73*, Univ. of Wales, Swansea (1973).
4. R. D. Wood and O. C. Zienckiewicz, 'Geometrically non-linear finite element analysis of beams, frames, arches and axisymmetric shells', *Comp. Struct.*, 7, 725–735 (1977).
5. E. Ramm, 'A plate/shell element for large deflections and rotations', in *Formulations and Computational Algorithms in Finite Element Analysis* (K. J. Bathe, J. T. Oden and W. Wunderlich, Eds) M.I.T. Press, 1977.
6. J. H. Argyris, H. Balmer, M. Kleiber and U. Hindenlang, 'Natural description of large inelastic deformations for shells of arbitrary shape—applications of trump element', *J. Comp. Meth. Appl. Mech. Eng.*, **22**, 361–389 (1980).
7. J. R. Hughes and W. K. Liu, 'Non-linear finite element analysis of shells—Part I. Three-dimensional shells', *J. Comp. Meth. Appl. Mech. Eng.*, **26**, 331–362 (1981).
8. J. R. Hughes and W. K. Liu, 'Non-linear finite element analysis of shells—Part II. Two-dimensional shells', *J. Comp. Meth. Appl. Mech. Eng.*, **27**, 167–181 (1981).
9. T. Y. Chang and K. Sawamiphakdi, 'Large deflection and post-buckling analysis of shell structures', *Comp. Meth. Appl. Mech. Eng.*, **32**, 311–326 (1982).

10. W. A. Cook, 'A finite element model for non-linear shells of revolution', *Int. J. numer. methods eng.*, **18,** 135–149 (1982).
11. K. S. Surana, 'Geometrically non-linear formulation for the axisymmetric shell elements', *Int. j. numer. methods eng.*, **18,** 477–502 (1982).
12. K. S. Surana, 'Geometrically non-linear formulation for the curved shell elements', *Int. j. numer. methods eng.*, **19,** 581–615 (1983).
13. J. L. Batoz and J. P. Jameaux, 'Large displacements and post-buckling of plane structures', Euromech colloquium No. 165, *Flexible Shells. Theory and Applications*, Munich, W. Germany, 1983.
14. K.-J. Bathe, *Finite Element Procedures in Engineering Analysis*, Prentice-Hall New Jersey, 1982.
15. J. Oliver and E., Oñate, 'A total Lagrangian formulation for the geometrically non-linear analysis of structures using finite elements. Part I. Two-dimensional problems: shell and plate structures', *Int. j. numer. methods eng.*, **20,** 2253–2281 (1984).
16. O. C. Zienckiewicz, *The Finite Element Method*, McGraw-Hill, New York, 1979.
17. M. Kleiber, J. A. Konig and A. Sawczuk, 'Studies on plastic structures: stability, anisotropic hardening, cyclic loads', *J. Comp. Meth. Appl. Mech. Eng.*, **33,** 487–556 (1982).
18. M. A. Crisfield, 'Incremental/iterative solution procedure for non-linear structural analysis', *Proc. Int. Conf. on Numerical Methods for non-linear Problems*, Swansea, Pineridge Press, Swansea, U.K., 1980.
19. D. J. Dawe, 'Finite deflection analysis of shallow arches by discrete element method', *Int. j. numer. methods eng.*, 3(4) (1971).
20. J. Oliver and E. Oñate, 'A finite element formulation for the analysis of marine pipeline during laying operations', *J. Pipelines*, **5,** 15–35 (1985).
21. J. Oliver, 'Una formulación cuasi-intrínseca para el estudio, por el método de los elementos finitos de vigas, arcos, placas y láminas sometidas a grandes corrimientos en régimen elastoplástico' (in Spanish), *Ph.D. thesis*, E. T. S. Ingenieros de Caminos, Universitat Politècnica de Catalunya, Spain (1982).
22. E. Oñate and J. Oliver, 'A total Lagrangian finite element formulation for the large displacement/large rotation analysis of 3D shells, arches and axisymmetric shells', in *Numerical Methods for Non-linear Problems* (C. Taylor, E. Hinton, D. R. J. Owen and E. Oñate, Eds), Pineridge Press, Swansea, U.K. 1982.